SENSITIVITY STUDY IN FINDING THE OPTIMAL SHAPE OF A GREEN OFFICE BUILDING

Weimin Wang[1], Radu Zmeureanu[2], Hugues Rivard[1]
[1]Department of Construction Engineering, ETS, Montreal
[2]Centre for Building Studies, Concordia University, Montreal
weimin_wa@yahoo.com zmeur@bcee.concordia.ca Hugues.Rivard@etsmtl.ca

ABSTRACT

This paper presents a sensitivity study of the optimal shape of an office building. The perturbed design parameters include window ratios, structural systems, and insulation levels. The building footprint is defined as a simple polygon with no intersection of non-consecutive edges. Thus, design variables are polygon-related parameters including the length and direction of each edge. Life cycle cost and life cycle environmental impact are two objective functions to be minimized simultaneously. The operating energy consumption is estimated with the aid of the ASHRAE Toolkit for building load calculations. Genetic algorithm is employed to solve the multi-objective optimization problem. The sensitivity study is carried out for a 1000 m^2 intermediate floor space of an office building in Montreal, with the shape of a pentagon.

INTRODUCTION

Shape is one of the most important considerations in the conceptual stage of building design. Since building shape determines the size and the orientation of exterior envelope exposed to the outdoor environment, it can affect building performance in many aspects such as environmental impact and life-cycle cost. In current practice, however, decisions on building shape are often based on aesthetics only. The decided shape is then passed along the building delivery process to engineering professionals who are responsible for the technical implementation of that scheme. The conventional decision-making procedure on building shape has the evident disadvantage of limiting the potential of performance improvement. This disadvantage can be addressed by pursuing shape optimization in the conceptual stage of design in terms of both environmental and economical performance.

Several studies (e.g., Bouchlaghem 2000; Peippo et al. 1999) assumed a rectangular building plan and optimized its geometry via aspect ratio. Jedrzejuk and Marks (2002) optimized a building with a symmetrical octagonal plan. Wang et al. (2005a) considered both L-shape and rectangular shape for the optimization of green building design. All previous studies considered only simple shapes that cannot be easily generalized. Moreover, since these shapes are heavily constrained, more promising shapes could be precluded from the design space initially.

This paper uses a generalized polygon representation for shape optimization considering two conflicting criteria: minimum life-cycle cost and minimum life-cycle environmental impact. The paper is organized as follows. The shape representation and implementation methods are discussed in the next section. The optimization problem is formulated in the third section with the investigated cases for the sensitivity study. Then, the results are presented and discussed.

SHAPE REPRESENTATION AND IMPLEMENTATION

In this research, the footprint of a building is defined as a simple n-sided polygon with no intersection of non-consecutive edges. This geometrical shape is selected based on the following three considerations: (1) Since most energy simulation programs used to estimate building energy consumption cannot directly model curved surfaces, the line segments of a polygon facilitates the description of building geometry for application to those simulation programs; (2) Since a curve can be approximated with a large number of line segments, the polygon provides a basis to consider more complicated building shapes in the future; and (3) Since real buildings do not have intersected boundary, it is reasonable to limit the scope to simple polygons. For a given area, an n-sided polygon can be determined in different ways depending how its edges are defined. In this paper, one edge of a polygon is defined by its length and bearing, where the bearing is the angle between a designated north direction (e.g., the true north indicated by a compass) and the edge, clockwise positive. The general procedure to establish an n-sided polygon with the length-bearing method requires the following steps (Figure 1):

- Starting from a point P_1, the endpoint P_2 of the first edge can be determined according to its length a_1 and bearing α_1.

- The endpoint P_{i+1} of the *i-th* edge can be determined based on its starting point (i.e., P_i), its length a_i and bearing α_i.
- The previous step is repeated until the point P_{n-1} is defined. Then, given the bearing of the *(n-1)th* edge, the last point P_n can be defined to satisfy the area requirement.

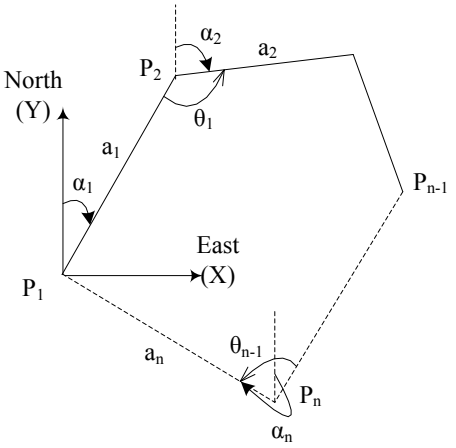

Figure 1: Length-bearing representation of a polygon

Therefore, with the length-bearing representation method, an n-sided polygon requires a total of $2*n-3$ independent variables including α_1, a_1, α_2, a_2,…, α_{n-2}, a_{n-2}, and α_{n-1}. These independent variables are used to determine the values of a_{n-1}, a_n and α_n.

Due to the requirement of a fixed area and the randomness of variable values generated in the optimization process, the above procedure cannot always result in a feasible simple polygon. The infeasibility may be due to the intersection of non-consecutive edges or the violation of design constraints. Thus, an algorithm is implemented to take the independent variables and to check the feasibility in constructing the polygon. The implemented algorithm contains the following eight steps:

Step 1: Calculate the edge angles θ_1, θ_2,…, θ_{n-2} according to Equation 1.

$$\theta_i = \begin{cases} 180+\alpha_i-\alpha_{i+1} & (-180 \le \alpha_i-\alpha_{i+1} \le 180) \\ 540+\alpha_i-\alpha_{i+1} & (\alpha_i-\alpha_{i+1} < -180) \\ -180+\alpha_i-\alpha_{i+1} & (\alpha_i-\alpha_{i+1} > 180) \end{cases} \quad (1)$$

where, α_i is the bearing of the *i-th* edge in degrees; θ_i is the angle in degrees evaluated in counter clockwise from the *i-th* to *(i+1)th* edge.

Step 2: Check whether all the edge angles θ_1, θ_2,…, θ_{n-2} fall into the predefined interval. If not, the solution is infeasible; otherwise, go to the next step.

The boundary values of the edge angle θ are usually defined to avoid creating tapered floor area that is difficult to be used in practice. For example, if a designer regards as unacceptable when the acute angle between two edges is less than 15 degrees, the interval of θ can be defined as between 15 and 345 degrees.

Step 3: Calculate the coordinates of vertices P_1, P_2, …, P_{n-1}.

Assuming that the Cartesian coordinate system has x-axis in the east direction and y-axis in the north direction and that the first vertex P_1 is located at the origin (x_1=0, y_1=0), the coordinates of other vertices can be defined with Equations 2 and 3.

$$x_{i+1} = x_i + a_i \cdot \sin\alpha_i \quad (2)$$

$$y_{i+1} = y_i + a_i \cdot \cos\alpha_i \quad (3)$$

where, a_i is the length of the *i-th* edge in meters for *i=1* to *n-2*.

Step 4: Check the first n-2 edges to see whether there exists intersection between two non-consecutive edges. If yes, the solution is infeasible; otherwise, go to the next step.

Step 5: Calculate the length of the *(n-1)th* edge: a_{n-1}.

According to Equations 3 and 4, the coordinates of the last vertex P_n can be expressed as:

$$x_n = x_{n-1} + a_{n-1} \cdot \sin\alpha_{n-1} \quad (4)$$

$$y_n = y_{n-1} + a_{n-1} \cdot \cos\alpha_{n-1} \quad (5)$$

Depending on the order of its vertices, the area of a polygon can be calculated with the following equation (O'Rourke 1998):

$$S = \frac{1}{2}\left|\sum_{i=1}^{n}(x_i y_{i+1} - y_i x_{i+1})\right| \quad (6)$$

where, S is the given floor area in m^2; $x_{n+1} = x_1 = 0$ and $y_{n+1} = y_1 = 0$.

Substituting x_n and y_n in Equation 6 by their expressions in Equations 4 and 5, only a_{n-1} is unknown and it can be solved.

Step 6: Check whether the last two edges intersect with any of their non-consecutive edges from a_1 to a_{n-2}. If yes, the solution is infeasible; otherwise, go to the next step.

Step 7: Calculate the last edge length a_n and the last two edge angles: θ_{n-1} and θ_n.

With a_{n-1} obtained from the fifth step, the coordinates of the last vertex can be derived from Equations 4 and 5. Based on the coordinates of the two vertices P_1 and P_n, the edge length a_n can be calculated. The value of a_n is then used to calculate the bearing of the last edge (α_n) with Equations 2 and 3. Since the bearings of all edges are known by now, the edge angles θ_{n-1} and θ_n can be derived from Equation 1.

Step 8: Check the validity of the values obtained in the previous step.

If any of these values lie out of their intervals, the solution is infeasible; otherwise, the polygon represents a feasible building plan satisfying all predefined geometrical constraints.

PROBLEM FORMULATION

The design of a multi-story office building located in Montreal, Canada, is employed in this paper to formulate the optimization problem. The building takes the shape of a pentagon. The floor-to-floor height is 3.6 m. Since this study focuses on two-dimensional shape optimization, only one typical floor is considered. The typical floor has an area of 1000 m^2. In the energy simulation program, the heating season is from November to March, and the cooling season from June to August. The indoor design temperatures are 21°C for heating and 23°C for cooling, without night setback or setup. Internal loads and daily operating schedule take the default values for office buildings according to the Model National Energy Code of Canada for Buildings (National Research Council 1997). A period of 40 years is used in the life-cycle analysis for building performance.

The following two objective functions must be minimized in this research: the life-cycle cost (LCC) and the life-cycle environmental impact (LCEI). Let X denotes a vector of variables. The general expressions to calculate LCC ($) and LCEI (MJ) are:

$$\text{Min: } \mathrm{LCC}(\mathbf{X}) = \mathrm{IC}(\mathbf{X}) + \mathrm{OC}(\mathbf{X}) \quad (7)$$

$$\text{Min: } \mathrm{LCEI}(\mathbf{X}) = \mathrm{EE}(\mathbf{X}) + \mathrm{OE}(\mathbf{X}) \quad (8)$$

where, *IC* is the initial construction cost ($) of the considered components such as exterior walls, windows, and overhangs; *OC* is the present worth of life-cycle operating costs ($) that comprise energy consumption cost and peak demand cost; *EE* is the environmental impact (MJ) due to building construction; *OE* is the environmental impact (MJ) due to building operation for heating, cooling and lighting.

In this study, the environmental impact of a building is evaluated with the "expanded cumulative exergy consumption" (Wang et al. 2005b). This indicator consists of two items: the cumulative exergy consumption and the abatement exergy consumption. The first item expresses the sum of exergy of all natural sources consumed by a building throughout its whole life-cycle covering the operation phase and the pre-operation phase (including resource extraction, building material production, on-site construction, operation, and transportation between the above processes). The second item is the exergy required by necessary operations if the wastes produced in the life-cycle phases of a building are removed or recovered to ensure their releases to the environment at acceptable levels. The wastes considered here focus on emissions to air, including three major greenhouse gases (CO_2, CH_4, N_2O) and two major acidic gases (SO_x and NO_x). Therefore, the environmental impact EE and OE in Equation 8 represents the expanded cumulative exergy consumption in the pre-operation phase and operation phase, respectively. A simulation program based on the ASHRAE toolkit for building load calculations (Pedersen et al. 2000) has been developed to calculate the two objective function values. The data for computing the initial construction costs and the embodied environmental impacts are mostly obtained from RS. Means (2004) and the ATHENA software (2003), respectively. A detailed description of this simulation program and its sources of data can be found in (Wang et al. 2005b).

For the pentagon floor, the variables to be optimized include the edge lengths a_1 to a_3 and the bearings α_1 to α_4. The interval of each edge length is set between 5 and 200 m and the interval of each edge angle is set between 15 and 345 degrees.

The purpose of this research is to investigate the change of the optimal shape and its associated performance with window ratios, structural systems, and insulation levels. Therefore, these design parameters are perturbed gradually to form a series of optimization problems. The window ratio has four levels: 0.2, 0.4, 0.6, and 0.8. The same window ratio applies to all facades and low-e (emissivity=0.1) double glazing with coating on the exterior of the inside pane is the considered window type. The structural system has two options: steel frame and concrete frame. The two structural systems use the same steel-stud wall type; however, they have different floor types: steel deck on open web steel joist for the steel frame and cast-in-place concrete for the concrete frame. The steel-stud wall consists of brick veneer, rigid insulation, sheathing paper, gypsum sheathing, 100 mm wide steel-stud with cavity insulation, vapor barrier, and gypsum board. The rigid insulation uses extruded polystyrene (XPS) with two different thickness values: 76 mm and 152 mm, respectively standing for normal and high

insulation levels. The overview of investigated cases is presented in Table 1.

Table 1: Overview of cases for the sensitivity study

cases	window ratio	insulation	structural system
1-4	0.2, 0.4, 0.6, 0.8	76 mm XPS	steel
5-6	0.2, 0.8	152 mm XPS	steel
7-10	0.2, 0.4, 0.6, 0.8	76 mm XPS	concrete
11-12	0.2, 0.8	152 mm XPS	concrete

The multi-objective genetic algorithm presented in (Wang et al. 2005b) is employed here to solve the formulated optimization problems. A major advantage of multi-objective genetic algorithm lies in its ability to locate multiple Pareto optimal solutions in a single run. A solution is said to be Pareto optimal if and only if it is not dominated by any other solution in the performance space. If solution $\mathbf{X_1}$ dominates another solution $\mathbf{X_2}$, it implies that $\mathbf{X_1}$ is non-inferior to $\mathbf{X_2}$ for all the considered performance criteria but it is better than $\mathbf{X_2}$ for at least one criterion. All Pareto solutions form a Pareto front in the performance space. The results are presented and analyzed next.

RESULTS AND DISCUSSION

Figures 2 and 3 show the Pareto fronts for cases 1-4 (steel-frame structure) and 7-10 (concrete-frame structure), from which the following observations can be derived:

- With increasing the window ratio, both LCC and LCEI increase. In addition, the size of Pareto fronts increases with the window ratio.
- The Pareto front for the concrete structure (Figure 3) is much longer than the corresponding one for the steel structure (Figure 2).
- The Pareto fronts for different window ratios lie in between two straight lines, the equations of which are obtained through linear correlation based on the function values of the edge points of the fronts.

In addition to modeling the relationship between LCEI and LCC for the edge points of the Pareto fronts, the relationship between the extreme function values and the window ratio can be also modeled. For example, Table 2 lists the extreme function values for cases 1-4 with steel structure and the corresponding linear regression models. Since the coefficient of determination R^2 is close to 1, there is a strong linear relationship between window ratio and the extreme values of LCC or LCEI. Similar strong linear relationships also exist for the cases with the concrete-frame structure.

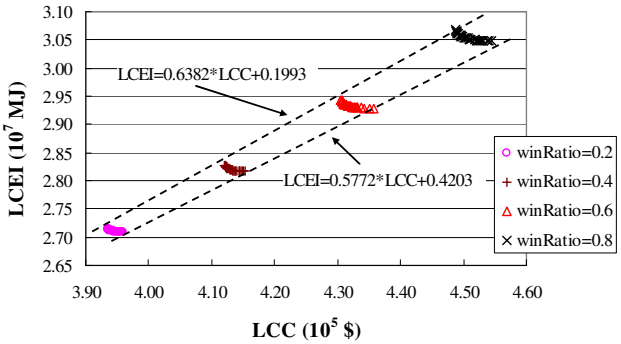

Figure 2: Pareto fronts and the boundary linear equations for cases 1-4 (steel-frame structure)

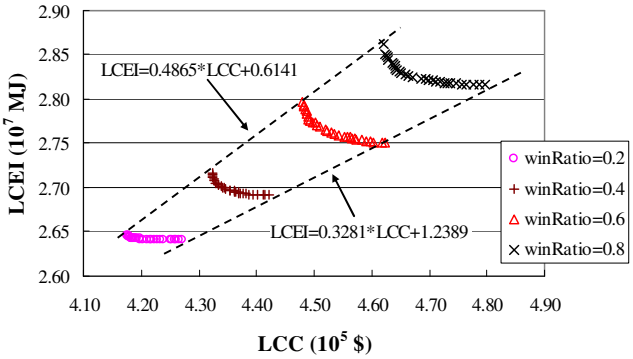

Figure 3: Pareto fronts and the boundary linear equations for cases 7-10 (concrete-frame structure)

Due to the large number of optimal solutions that are obtained from 12 cases in Table 1, a particular case is selected for further analysis of the optimal values of variables. Table 3 lists the Pareto solutions from case 10 (concrete frame, window ratio=0.8, 76 mm XPS). The solutions are arranged in increasing order of the life-cycle cost. To facilitate the following discussion, Table 3 presents not only the values of independent variables but all the edge bearings, lengths, and the corresponding function values. The perimeter is also indicated in that table because it is a valuable indicator to measure the compactness of a building with fixed floor area and height. The shapes of the first and last solutions are respectively illustrated in Figures 4 (a) and (b). Results are briefly explained below.

- The increase of perimeter leads to the increase of the life-cycle cost and the life-cycle environmental impact. The solutions with lower LCC have their perimeters close to that of the regular pentagon (perimeter=120.5 m). For example, the first solution has a perimeter of 121.6 m. The solutions with lower LCEI have

larger edge length (a_5) on the south façade in order to take advantage of the solar-heating effect for the cold climate in Montreal.

- Since a fixed floor area is maintained, the increasing of perimeter and edge length a_5 must be accompanied by the changes of other edges. As can be seen from Figures 4 (a) and (b), façade 2 is north-east-oriented; façade 3 is north-oriented; and facade 4 is mainly west-oriented. Therefore, the most significant changes exist in α_2, α_4 and a_4 in order to reduce the unfavorable solar effect in summer morning and afternoon. There is a little change only on the edge 3 because the solar radiation has minor impact on the north-oriented facade.

The variables take different optimal values for different cases. There is no observable relationship between window ratio and edge lengths or bearings. Although the rule that perimeter increases with the LCC holds for all cases, the degree of perimeter changes is different for the two structural systems. The perimeter increases from about 121 to 126 m for the first six cases with the steel structure and from 121 to 140 m for the last six cases with the concrete structure. This difference indicates that the Pareto solution with minimum LCC always has its footprint close to a regular polygon but the solution with minimum LCEI has a more elongated footprint for the concrete structure. For example, Figures 4 (c) and (d) show the footprints of the two solutions with minimum LCC and LCEI for case 4 (steel frame, window ratio=0.8, 76 mm XPS). It is clear that in Figure 4, both (a) and (c) are close to a regular pentagon while (b) is more elongated along the east-west than (d). In order to verify the above difference, the original solution in Figure 4 (d) is replaced by the shape in Figure 4 (b) and its performance is investigated. Simulation shows that the perturbed solution has its function values as: LCC=$4.712*10^5$ \$ and LCEI=$3.074*10^7$ MJ, which is dominated by the original solution. The fact that a building with concrete structure takes more diversified footprints can explain why the Pareto fronts in Figure 3 are longer than those in Figure 2.

Figure 5 compares the Pareto fronts for the two predefined insulation levels. This figure leads to the following observations:

- For a building with low window ratio (e.g., 0.2), all solutions with normal and high insulation levels are non-dominated with each other for the steel structure (Figure 5, a); however, solutions with the high insulation level may dominate some with normal insulation level for the concrete structure (Figure 5, c).
- For a building with high window ratio (e.g., 0.8), whatever the structural system is, the normal insulation level performs better than the high insulation level for the solutions favorable for the cost performance on the upper part of fronts, while the situation is inverse for the solutions favorable for the environmental performance on the lower part of fronts (Figure 5, b and d).

CONCLUSION

The sensitivity study has shown that the Pareto fronts for different window ratios basically lie in two straight lines in the performance space. A strong linear relationship exists between the extreme function values and the window ratio. Perimeters increase for the solutions from the upper to the lower part of the Pareto front. The Pareto solutions have more diversified shapes for a concrete-frame building than those for a steel-frame building. Depending on the window ratio and structural system, increasing insulation level may not lead to the improvement of the optimal solutions.

Since the length-bearing method is a generalized representation method for two-dimensional shape optimization of green building design, similar optimization problems with different number of sides can be solved and the results are compared with the current study.

ACKNOWLEDGEMENTS

The authors gratefully acknowledged the financial support received by Dr. H. Rivard from the FQRNT (Fonds québécois de la recherche sur la nature et les technologies) and the Canada Research Chair titled Computer-Aided Engineering for Green Building Design.

REFERENCES

ATHENA EIE Version 3.0. 2003. The ATHENA sustainable materials institute, Ottawa, Canada,

Bouchlaghem N. 2000. Optimizing the design of building envelopes for thermal performance. *Automation in Construction* 10(1), 101-112.

Jedrzejuk H., Marks W. 2002. Optimization of shape and functional structure of buildings as well as heat source utilization: Partial problems solution. *Building and Environment* 37(11): 1037-1043.

National Research Council. 1997. Model National Energy Code of Canada for Buildings, Ottawa, Canada.

O'Rourke J. 1998. Computational geometry in C. 2nd edition. Cambridge, UK: Cambridge University Press.

Pedersen C.O., Liesen R.J., Strand R.K., Fisher D.E., Dong L., Ellis P.G. 2000. A Toolkit for Building Load Calculations, ASHRAE.

Peippo K., Lund P.D., Vartiainen E. 1999. Multivariate optimization of design trade-offs for solar low energy buildings. *Energy and Building* 29(2): 189-205.

RS Means. 2004. Building construction cost, Kingston, MA.

Wang W., Rivard H., Zmeureanu R. 2005a. An object-oriented framework for simulation-based green building design optimization with genetic algorithms. *Advanced Engineering Informatics* 19(1): 5-23.

Wang W., Zmeureanu R., Rivard H. 2005b. Applying multi-objective genetic algorithms in green building design optimization. *Building and Environment* 40(11): 1512-1525.

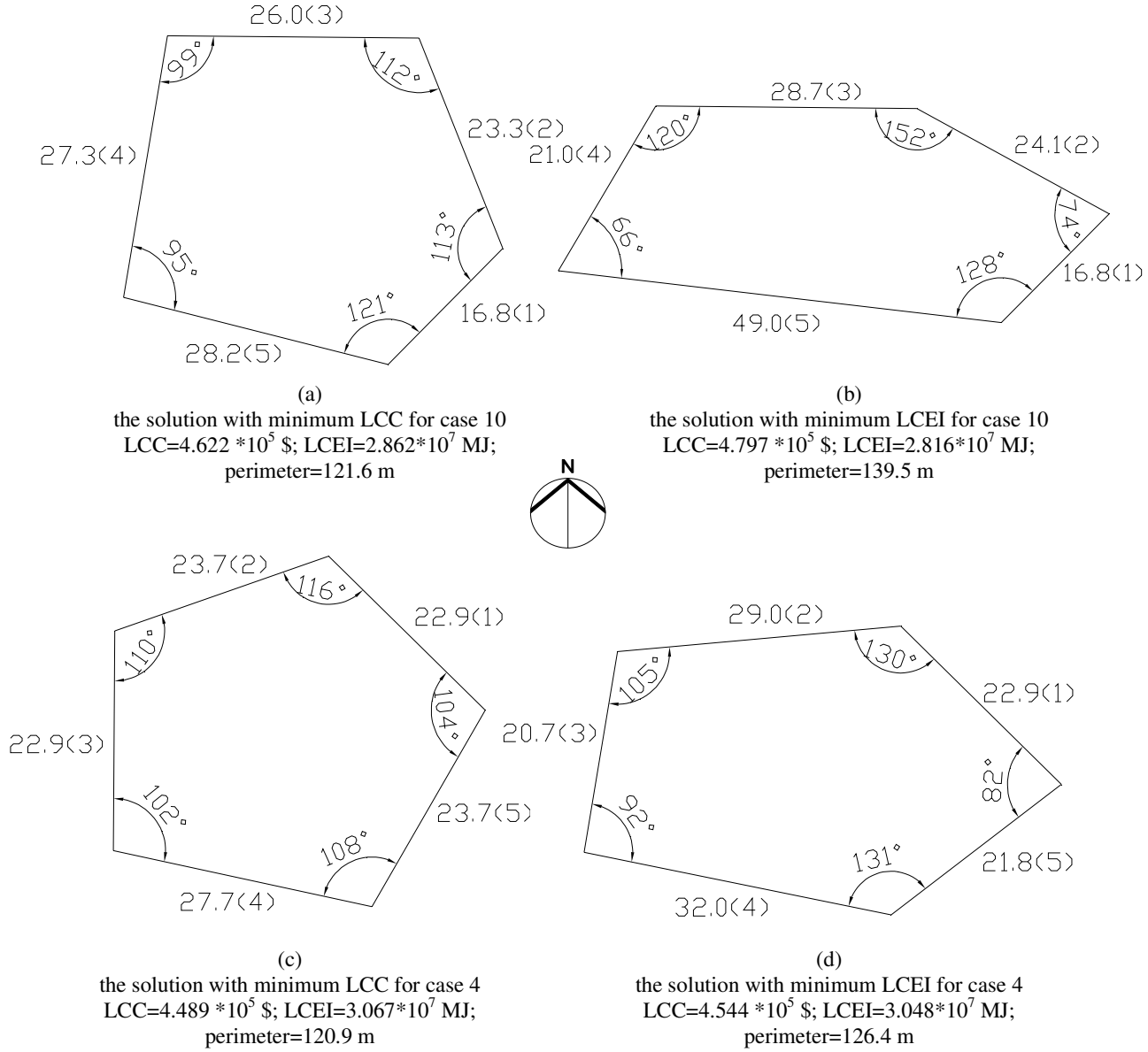

(a)
the solution with minimum LCC for case 10
LCC=4.622 *10^5 $; LCEI=2.862*$10^7$ MJ;
perimeter=121.6 m

(b)
the solution with minimum LCEI for case 10
LCC=4.797 *10^5 $; LCEI=2.816*$10^7$ MJ;
perimeter=139.5 m

(c)
the solution with minimum LCC for case 4
LCC=4.489 *10^5 $; LCEI=3.067*$10^7$ MJ;
perimeter=120.9 m

(d)
the solution with minimum LCEI for case 4
LCC=4.544 *10^5 $; LCEI=3.048*$10^7$ MJ;
perimeter=126.4 m

Figure 4: Building footprints of selected solutions. The numbers in the parentheses indicate edge indices

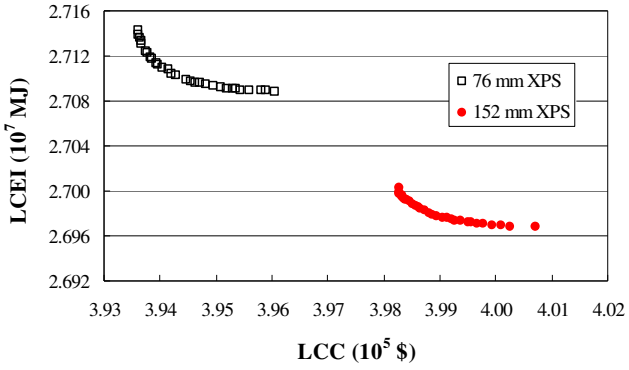

(a)
steel-frame structure, window ratio=0.2

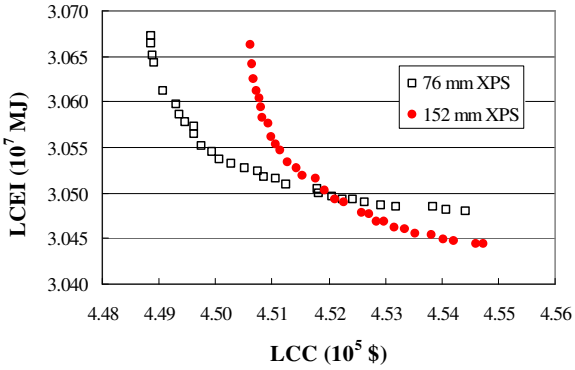

(b)
steel-frame structure, window ratio=0.8

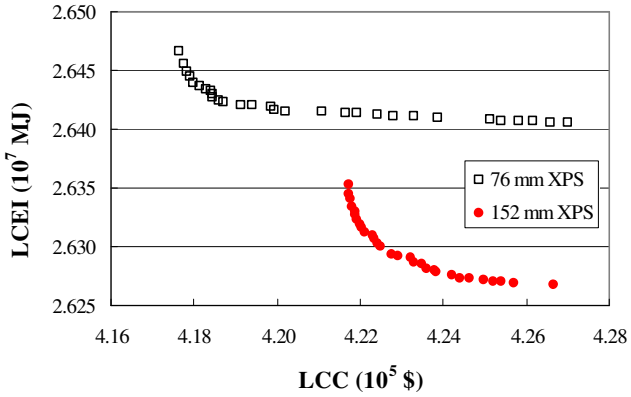

(c)
concrete-frame structure, window ratio=0.2

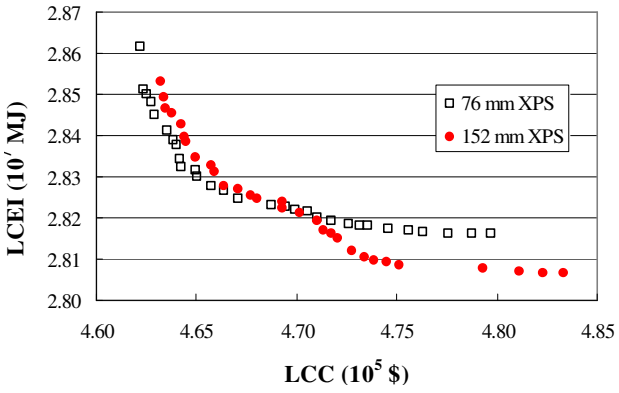

(d)
concrete-frame structure, window ratio=0.8

Figure 5: Comparison of Pareto fronts for different insulation levels

Table 2:Data and results for the linear regression between extreme function values and window ratio (for cases 1-4 with steel-frame structure and 75 mm XPS insulation)

response (y)		window ratio (x)				linear regression	
		0.2	**0.4**	**0.6**	**0.8**	**model**	**R^2**
LCC (10^5 \$)	Min.	3.936	4.121	4.306	4.489	y=0.9212x+3.7522	≈1
	Max.	3.961	4.153	4.358	4.544	y=0.9781x+3.7648	≈1
LCEI (10^7 MJ)	Min.	2.709	2.817	2.929	3.048	y=0.5648x+2.5932	≈1
	Max.	2.714	2.827	2.944	3.067	y=0.5879x+2.5941	≈1

Table 3:Pareto solutions for case 10

ID	edge bearing (degree)					edge length (m)					perimeter (m)	LCC (10^5 \$)	LCEI (10^7 MJ)
	1	**2**	**3**	**4**	**5**	**1**	**2**	**3**	**4**	**5**			
1	45	338	271	190	104	16.8	23.3	26.0	27.3	28.2	121.6	4.622	2.862
2	41	338	271	190	103	16.8	20.3	29.0	25.5	30.6	122.2	4.624	2.851
3	41	338	271	192	104	16.8	20.3	29.0	24.7	31.5	122.4	4.625	2.850
4	43	330	271	190	102	16.1	23.3	26.0	25.7	31.7	122.8	4.628	2.848
5	45	327	271	190	103	16.8	23.3	26.0	25.2	31.8	123.1	4.629	2.845
6	43	322	271	190	100	16.8	23.3	25.2	25.7	32.7	123.8	4.635	2.841
7	43	322	271	190	101	16.4	23.3	26.0	24.7	33.7	124.2	4.639	2.839
8	45	322	271	192	102	16.8	23.3	26.0	24.2	34.1	124.4	4.640	2.838
9	45	327	271	194	103	16.8	21.0	29.0	22.6	35.2	124.7	4.642	2.834
10	43	324	271	192	99	16.8	20.3	29.0	24.1	34.6	124.9	4.642	2.832
11	40	321	271	193	101	16.8	20.3	29.0	22.7	36.7	125.5	4.649	2.831
12	40	318	271	190	98	16.8	20.3	29.0	23.6	36.0	125.7	4.650	2.830
13	41	317	271	192	98	16.8	20.3	29.0	23.3	36.9	126.4	4.657	2.828
14	43	316	271	192	95	16.8	20.3	29.0	24.3	36.7	127.1	4.664	2.827
15	44	316	271	195	96	16.8	20.3	29.0	23.7	37.9	127.8	4.671	2.825
16	43	311	271	190	97	15.7	23.3	28.7	22.1	39.5	129.3	4.687	2.823
17	43	311	271	198	99	16.1	23.3	27.5	21.7	41.4	130.0	4.695	2.823
18	43	311	271	199	98	15.7	23.3	27.5	21.9	42.1	130.5	4.699	2.822
19	44	305	271	187	94	16.1	23.3	29.0	22.9	39.7	131.0	4.706	2.821
20	44	305	271	190	94	16.1	23.3	29.0	22.4	40.8	131.6	4.710	2.820
21	43	302	271	190	94	16.8	23.3	29.0	22.1	41.0	132.2	4.718	2.819
22	43	305	271	199	96	16.1	23.3	28.3	21.6	43.8	133.1	4.726	2.819
23	45	305	271	201	96	16.1	23.3	28.3	21.9	44.0	133.6	4.732	2.818
24	44	302	271	198	97	16.8	24.1	28.3	21.0	43.7	133.9	4.736	2.818
25	44	302	271	199	98	16.8	24.1	29.0	20.1	44.8	134.8	4.746	2.817
26	43	302	271	205	98	16.8	23.3	29.0	20.4	46.3	135.8	4.756	2.817
27	44	299	271	201	96	16.8	24.1	29.0	20.6	45.9	136.5	4.764	2.817
28	44	299	271	205	97	16.8	24.1	29.0	20.4	47.3	137.6	4.776	2.816
29	44	300	271	211	98	16.8	24.1	28.7	20.4	48.7	138.6	4.788	2.816
30	45	299	271	211	97	16.8	24.1	28.7	21.0	49.0	139.5	4.797	2.816